Journal of Magnetism and Magnetic Materials 389 (2015) 73–76

Contents lists available at ScienceDirect

Journal of Magnetism and Magnetic Materials

journal homepage: www.elsevier.com/locate/jmmm

Electronic structure and magnetism on FeSiAl alloy: A DFT study

V. Cardoso Schwindt, M. Sandoval, J.S. Ardenghi, P. Bechthold, E.A. González, P.V. Jasen *

Departamento de Física, Universidad Nacional del Sur & IFISUR (UNS-CONICET), Av. Alem 1253, 8000 Bahía Blanca, Argentina

ARTICLE INFO

Article history:
Received 12 January 2015
Received in revised form
6 April 2015
Accepted 9 April 2015
Available online 11 April 2015

Keywords:
Fe–Si–Al alloy
DFT
Soft magnetic properties
Magnetic materials

ABSTRACT

Density functional theory (DFT) calculation has been performed to study the electronic structure and chemical bonding in FeSiAl alloy. These calculations are useful to understand the magnetic properties of this alloy. Our results show that the mean magnetic moment of Fe atoms decreases due to the crystal structure and the effect of Si and Al. Depending on the environment, the magnetic moment of one Fe site (Fe_1) increases to about 14.3% while of the other site (Fe_2) decreases to about 25.9% (compared with pure bcc Fe). All metal–metal overlap interactions are bonding and slightly weaker than those found in the bcc Fe structure. The electronic structure (DOS) shows an important hybridization among Fe, Si and Al atoms, thus making asymmetric the PDOS with a very slight polarization of Al and Si atoms. Our study explains the importance of crystal structure in determining the magnetic properties of the alloys. FeSiAl is a good candidate for electromagnetic interference shielding combining low price and good mechanical and magnetic properties.

1. Introduction

With the exponential growth of the mobile communication and computer technologies in the past three decades, the need of high-speed data transmission systems also grew. This kind of technology involves the use of microwaves of ultra high frequency (UHF) in the range of 0.3–3 GHz and super high frequency (SHF) in the range of 3–30 GHz. As a result, our environment is actually polluted by these electromagnetic waves of high frequencies. The risk posed by these high frequencies to human health and electrical equipment has drawn the interest of many researchers, who started to investigate different materials for the development of wave absorbers for this particular range of frequencies [1–4].

Electromagnetic interference (EMI) shielding offers an effective way to deal with wave-polluted environments. Conventional microwave absorption materials used for this purpose are typically made of metal powders such as iron, cobalt, nickel, metal alloys and ferrites. These materials present the drawback of being expensive and quite heavy, which restricts their use in applications requiring low price and lightweight mass. The conventional shielding materials fixed on electronic devices may interfere with the electrical circuits.

The manufacturing of absorbing/shielding materials with "thin, lightweight, wide, and strong" characteristic will efficiently overcome the above mentioned problems. Incident microwaves are attenuated thanks to these materials and the microwaves reflected become much weaker as compared to the incident waves reflected from traditional shielding materials [5].

Fe_3Si and Fe_3Al alloys have excellent soft magnetic properties and they are widely used in different applications. Although these two alloys are isomorphous, they present very different mechanical properties; Fe_3Si is brittle, whereas Fe_3Al is ductile [6]. In order to improve their mechanical and magnetic properties, researchers have mixed these two binary alloys into FeSiAl. Many authors have reported important changes in the structural and magnetic properties of this new alloy compared to the Fe_3Si and Fe_3Al. Legarra et al. [7] reported that the Si substitution on the FeAl prevents the disorder of the alloy. FeAlSi crystallizes in the DO3-type structure [8,9]. The crystal structure is very important in determining the magnetic properties of the alloys. The effect of Si in the FeAl alloys is twofold; Si contributes to the decrease of the lattice parameter which, as reported by Nogues et al. [10], is of major importance for the magnetism, and, on the other hand, having one more p electron than the Al atom promotes the charge transfer from Si to Fe atoms, as reported by Legarrara et al. [11]. These two effect make the magnetism decrease: lattice parameter decrease makes the magnetism weaker due to the decrease in the charge transfer between the Al–Si and Fe atoms. The introduction of an additional electron from Si makes the hybridization higher getting a lower magnetic moment [12].

The dependence of dynamic magnetization, magneto-transport properties and thermal stability of FeAlSi films with oblique sputtering was studied via spin rectification effect [13,14].

Mössbauer spectroscopy was used to understand the enhanced

* Corresponding author. Fax: +54 291 4595142.
E-mail address: pjasen@uns.edu.ar (P.V. Jasen).

http://dx.doi.org/10.1016/j.jmmm.2015.04.047
0304-8853/

microwave permeability of Fe–Si–Al particles. This study reveals that flaky particles have an average magnetic moment of 1.63 μ_B [15].

The aim of the present work is to analyze the electronic, band structure and chemical bonding of the FeSiAl alloy and to compare it with the results obtained for the pure bcc Fe.

2. Calculation methods and models

The FeSiAl alloy has DO3-type crystal structure, as shown in Fig. 1a, which is composed of four interpenetrating fcc lattices shifted by 1/4th of the main diagonal. These sublattices are abbreviated as A, B, C and D and originated at (0, 0, 0), (1/2, 1/2, 1/2), (1/4, 1/4, 1/4), (3/4, 3/4, 3/4). The A and C sublattices are symmetrically equivalent in DO3-type structure [6,16].

First principles calculations were performed using density functional theory (DFT) as implemented in the VASP code [17–19]. The exchange and correlation energies were calculated with the Perdew–Burke–Ernzerhof form of the spin-polarized generalized gradient approximation (GGA-PBE) [20]. Spin-polarization and non-linear core corrections [21] were included in the calculations for systems with Fe to correctly account for its magnetic properties. The electron–ionic core interaction was represented by ultrasoft pseudopotentials [22]. Valence atomic configurations are $3d^64s^2$ for Fe, $3s^23p^1$ for Al and $3s^23p^2$ for Si atom. A plane-wave basis with energy cutoff of 380 eV was used to expand the electronic wave functions. Brillouin zone integrations were performed on a $12 \times 12 \times 12$ special k-points mesh generated by the Monkhorst–Pack scheme [23]. In order to accelerate the convergence, for fractional occupancies the first order Methfessel–Paxton [24] method with the Fermi surface smearing of 0.2 eV was adopted. The positions of all atoms were fully optimized until the forces on each atom were less than 0.02 eV/Å. Test calculations for denser k-point meshes do not show significant improvement. The crystal structure was simulated using a 2-atom unit-cell for bcc Fe and a 16-atom unit-cell for the FeSiAl. Calculations for the lattice constant of bcc Fe give a value of 2.846 Å (2.867 Å, [25]), and the bulk modulus of 167 GPa (170 GPa, [25]) in a very good agreement with experimental data (quoted in the parenthesis). In addition, the local spin magnetic moment of 2.24 μ_B (Bohr magneton) for bcc Fe is in excellent agreement with previous calculations [26,27]. The approach used here is similar to that reported by Hung et al., giving a good description of bulk properties of bcc Fe [28]. In the case of the FeSiAl DO3 crystal structure the calculated lattice constant is 5.750 Å, which is in the range of values reported in the literature [12]. Bader analysis was used to calculate magnetic moments and electronic structure [29].

In order to understand the metal–metal interactions we have used the concept of density of states (DOS) and crystal orbital overlap population (COOP). The DOS curve is a plot of the number of orbitals as a function of the energy. The integral of the DOS curve over an energy interval gives the number of one-electron states in that interval; the integral up to the Fermi level (E_F) gives the total number of occupied molecular orbitals. If the DOS is weighed with the overlap population between two atoms the crystal orbital overlap population COOP is obtained. The integration of the COOP curve up to E_F gives the total overlap population of the specified bond orbital and it is a measure of the bond strength. If an orbital at certain energy is strongly bonded between

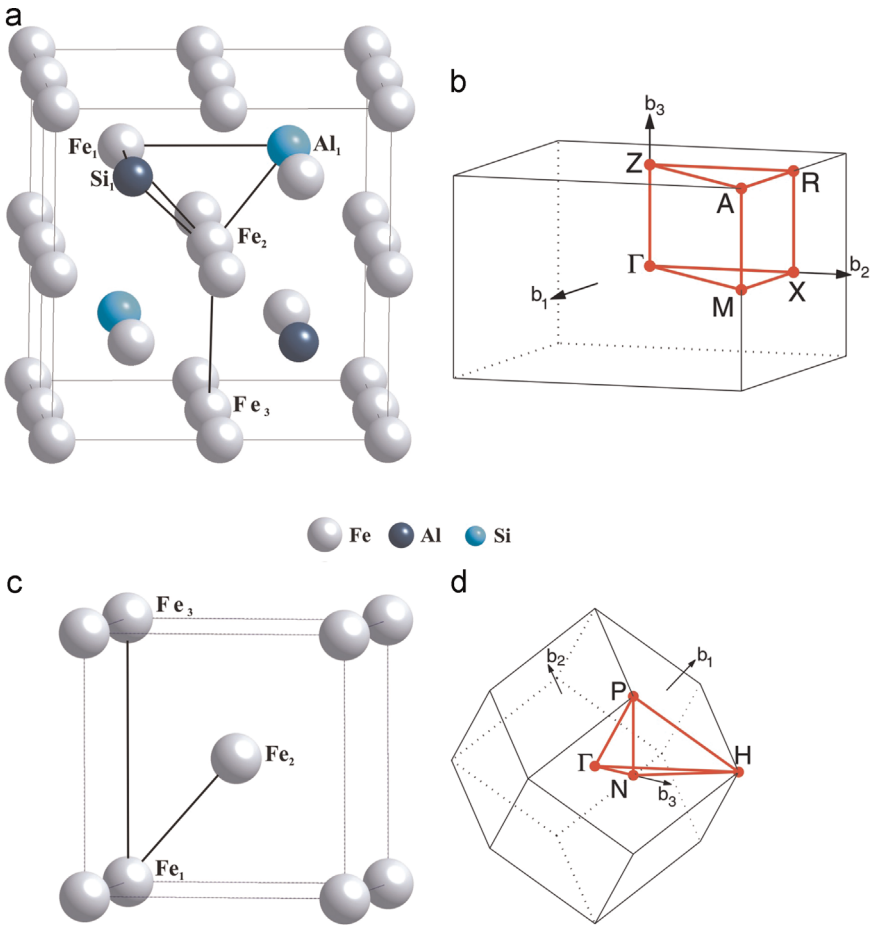

Fig. 1. Crystal structure and reciprocal space of FeSiAl (a, b) and bcc Fe (c, d).

two atoms, the overlap population is strongly positive and COOP curve will be large and positive around that energy. Similarly, the negative COOP around certain energy corresponds to antibonding interactions. The COOP curves were computed using the SIESTA code [30,31].

3. Results and discussion

We found that the cell volume and bulk modulus of DO3 FeSiAl are 190.11 Å^3 and 189.67 GPa, respectively; these values are in good agreement with those reported by Ma et al. for the $Fe_3Al_xSi_{1-x}$ alloy [6]. In this structure, there are two non-equivalent Fe positions, one surrounded by eight Fe atoms and the other surrounded by four Fe atoms denoted as Fe_1 and Fe_2, respectively (see Fig. 1a). The magnetic moments for the Fe_1 increase to 14.3% (from 2.24 to 2.56 μ_B) with respect to an Fe atom in the pure bcc iron structure, while for the Fe_2 decrease to 25.9% (from 2.24 to 1.66 μ_B). Hans and Deng recently measured an average magnetic moment in Fe–Si–Al particles of about 1.63 μ_B [15]. The saturation magnetic moment per unit cell is 23.26 μ_B. This behavior is in agreement with experimental Mössbauer spectroscopy data for the $Fe_3Al_xSi_{1-x}$ alloy [32]. The mean magnetic moment of Fe atoms also decreases, this fact can be related to the DO3 structure that has 66.7% of Fe atoms in Fe_2 positions. The explanation for this different behavior in the local magnetic moments of Fe atoms is easy if we consider the local environment of the Fe sites and the relative affinity of Si and Al for Fe. The bands corresponding to the spin up and spin down electrons split apart due to the exchange coupling between the electrons (see Fig. 2a, compare the black line with the red dashed line). The band structure of the crystal was computed along the symmetry lines $\Gamma \rightarrow X$; $X \rightarrow M$; $M \rightarrow \Gamma$; $\Gamma \rightarrow Z$; $Z \rightarrow R$; $R \rightarrow A$; and $A \rightarrow Z$ (see Fig. 1b). In fact, the exchange splitting reflects the strength of exchange between the magnetic ions. For the calculations of statistical average values of the exchange splitting (Δ_x) 60 bands near of the Fermi level were considered. The values obtained for Δ_x are -1.43 eV and -2.02 eV for FeSiAl and bcc Fe, respectively. Ma et al. [6] found Δ_x of -1.16 eV for the related structure Fe_3AlSi; however, this value depends on how many bands are taken in the average. It can be seen that the introduction of Si and Al reduces Δ_x, which could result in a decrease of Curie temperature T_C as a consequence of the decreasing magnetic moments, relative to the pure Fe. The calculated Stoner factor is higher than 1, thus indicating a stable ferromagnetism.

DOS analysis showed that the total DOS (TDOS) between -10.1 eV and -5.0 eV is mostly due to the Si 3p and Al 3p orbital contribution. Between -5 eV and 2 eV the contribution to the TDOS is mostly due to the Fe 3d states (see Fig. 2b–d). Also, the bands near the Fermi level are formed mainly from transition metal d-states (see Fig. 2a). The projected DOS (PDOS) for the Fe atoms in Fig. 2c shows that the spin up and spin down

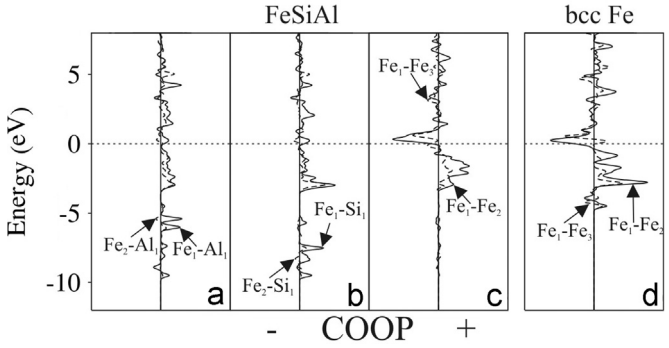

Fig. 3. COOP curves for FeSiAl. Fe–Al (a), Fe–Si (b) and Fe–Fe (c) bonds. COOP curves for Fe–Fe bonds in bcc Fe (d).

contributions are asymmetric, indicating that ferromagnetism is induced. The Fe_2 PDOS shows that the spin up contribution moves towards higher energy states and the spin down contribution is shifted to lower energy states (see Fig. 2c, full black line). The Fe_2 PDOS show hybridization due to the interaction with the Si and Al atom (see Fig. 2c, full black line between -10 eV and -5 eV). This interaction is also responsible for the decrease in the magnetic moment of Fe_2 atoms. We can see for the PDOS of Si and Al that the DOS spin up and spin down contributions are slightly shifted given a very small spin polarization (the magnetic moments for the Al and Si -0.057 μ_B and -0.066 μ_B, respectively).

Regarding the chemical bonding, the COOP curves presented in Fig. 3 shows almost all bonding regions. However, near to the Fermi level (E_F) the Fe–Fe interaction is antibonding.

The Fe–Fe distances are slightly elongated with respect to bcc Fe. The Fe–Fe OP decreases due to the Fe 3d interaction with the Al and Si sp orbitals (see Table 1).

4. Conclusions

Using periodic DFT calculations we have studied the FeSiAl alloy. This alloy presents two different sites of Fe atoms. The mean magnetic moment of Fe atoms decrease due to the crystal structure and the effect of Si and Al. Depending on the environment, the magnetic moment of one Fe site (Fe_1) increases to about 14.3% while of the other site (Fe_2) decreases to about 25.9% with respect to pure bcc Fe. The electronic structure (DOS) shows an important hybridization among Fe, Si and Al atoms, thus making asymmetric the PDOS with a very slight polarization of Al and Si atoms.

The DOS and band structure reveal stabilization of Fe, Si and Al bands. Almost all metal–metal interactions are bonding being the OP of Fe_1–Fe_2 and Fe_2–Fe_3 slightly lower to that computed for bcc Fe.

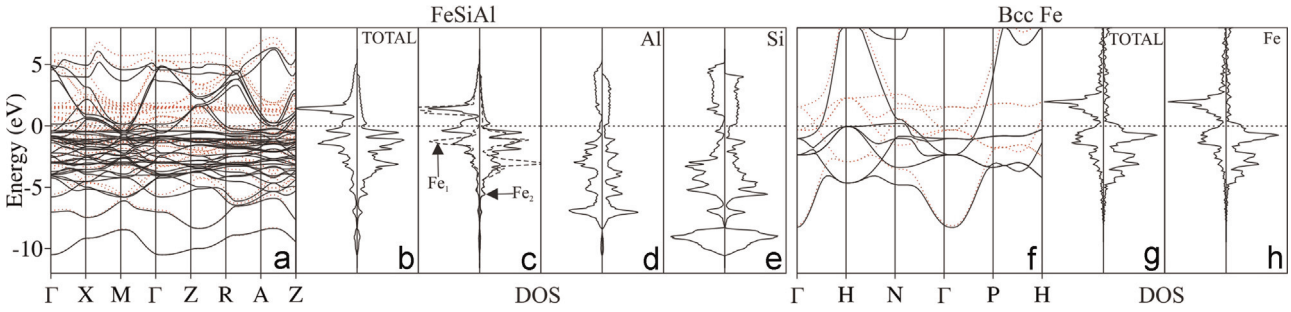

Fig. 2. Band structure (a) and TDOS (b) for FeSiAl. Fe_1 and Fe_2 (c), Al (d) and Si (e) PDOS. Band structure (f), TDOS (g) and Fe PDOS (h) of bcc Fe. (For interpretation of the references to color in this figure, the reader is referred to the web version of this article.)

Table 1
Electron orbital occupation, overlap population (OP), and distances for bcc Fe and FeSiAl crystal structures. The geometry is shown in Fig. 1.

Structure	Electron orbital occupation			Bond type	OP	Distance (Å)
	s	p	d			
Fe bcc						
Fe_1	0.68	0.24	5.53	Fe_1–Fe_2	0.286	2.477
				Fe_2–Fe_3	0.095	2.860
FeSiAl						
Fe_1	0.56	0.24	6.73	Fe_1–Fe_2	0.247	2.490
Fe_2	0.59	0.13	5.35	Fe_2–Fe_3	0.086	2.875
Al	1.73	1.27	–	Fe_2–Al	0.243	2.490
				Fe_1–Al	0.093	2.875
Si	1.41	1.85	–	Fe_2–Si	0.266	2.490
				Fe_1–Si	0.088	2.875

Acknowledgments

Our work was supported by SGCyT-UNS No. F058 and PICT No. 1770, PIP-CONICET Nos. 114-200901-00272 and 114-200901-00068. E. A. Gonzalez, P. V. Jasen and S. Ardenghi are members of CONICET. P. Bechthold is a fellow of CONICET. M. Sandoval is a fellow of ANPCyT. V. C. S. is fellow of CIC Pcia. Bs. As.

References

[1] Y. Cheng, J. Dai, X. Zhu, D. Wu, Y. Sun, Mater. Res. Bull. 45 (2010) 666–667.
[2] G. Li, G. Hu, H. Zhou, X. Fan, X. Li, Mater. Chem. Phys. 75 (2002) 101–104.
[3] K.-S. Zhou, H. Xia, K.-L. Huang, L.-W. Deng, D. Wang, Y.-P. Zhou, S.-H. Gao, Phys. B: Condens. Matter 404 (2009) 175–179.
[4] Z. Li, Y. Deng, B. Shen, W. Hu, Mater. Sci. Eng. B 164 (2009) 112–115.
[5] W. Yang, Y. Fu, A. Xia, K. Zhang, Z. Wu, J. Alloy. Compd. 518 (2012) 6–10.
[6] X.G. Ma, J.J. Jiang, S.W. Bie, L. Miao, C.K. Zhang, Z.Y. Wang, Intermetallics 18 (2010) 2399–2403.
[7] E. Legarra, E. Apiñaniz, F. Plazaola, J. Jimenez, R. Pierna, J. Magn. Magn. Mater. 320 (2008) e688–e691.
[8] T.J. Burch, K. Raj, P. Jena, J.I. Budnick, V. Niculescu, W.B. Muir, Phys. Rev. B 19 (1979) 2933–2938.
[9] L. Dobrzynski, C. Petrillo, F. Sacchetti, Phys. Rev. B 42 (1990) 1142–1149.
[10] J. Nogués, E. Apiñaniz, J. Sort, M. Amboage, M. d'Astuto, O. Mathon, R. Puzniak, I. Fita, J.S. Garitaonandia, S. Suriñach, J.S. Muñoz, M.D. Baró, F. Plazaola, F. Baudelet, Phys. Rev. B 74 (2006) 24407–24412.
[11] E. Legarra, F. Plazaola, J.S. Garitaonandia, D. Martín Rodriguez, J.A. Jimenez, Hyperfine Interact. 169 (2007) 1217–1222.
[12] E. Apiñaniz, E. Legarra, F. Plazaola, J.S. Garitaonandia, J. Magn. Magn. Mater. 320 (2008) e692–e695.
[13] W.T. Sho, X. Zhong, C.K. Ong, App. Phys. Lett. 105 (2014) (article no. 112401) (5 pages).
[14] X. Zhong, N.N. Phuoc, G. Chai, Y. Liu, C.K. Ong, J. Alloy. Compd. 610 (2014) 126–137.
[15] M. Han, L. Deng, J. Magn. Magn. Mater. 337–338 (2013) 70–73.
[16] T.D. Zhou, L.J. Deng, D.F. Liang, Acta Metall. Sin. (Engl. Lett.) 21 (2008) 191–196.
[17] G. Kresse, J. Hafner, Phys. Rev. B 47 (1993) 558–561.
[18] G. Kresse, J. Furthmüller, Phys. Rev. B 54 (1996) 11169–11186.
[19] G. Kresse, J. Furthmüller, Comput. Mater. Sci. 6 (1996) 15–50.
[20] J. Perdew, J. Chevary, S. Vosko, K. Jackson, M. Pederson, D. Singh, C. Fiolhais, Phys. Rev. B 46 (1992) 6671–6687.
[21] S. Louie, S. Froyen, M. Cohen, Phys. Rev. B 26 (1982) 1738–1742.
[22] D. Vanderbilt, Phys. Rev. B 41 (1990) 7892–7895.
[23] H. Monkhorst, J. Pack, Phys. Rev. B 13 (1976) 5188–5192.
[24] M. Methfessel, A. Paxton, Phys. Rev. B 40 (1989) 3616–3621.
[25] WebElements™ Periodic Table:⟨http://www.webelements.com/⟩.
[26] A. Stibor, G. Kresse, A. Eichler, J. Hafner, Surf. Sci. 507–510 (2002) 99–102.
[27] D. Jiang, E. Carter, Surf. Sci. 547 (2003) 85–98.
[28] A. Hung, I. Yarovsky, J. Muscat, S. Russo, I. Snook, R. Watts, Surf. Sci. 501 (2002) 261–269.
[29] R. Bader, Atoms in Molecules – A Quantum Theory, Oxford University Press, Oxford, USA, 1990.
[30] P. Ordejón, E. Artacho, J. Soler, Phys. Rev. B 53 (1996) R10441–R10444.
[31] J. Soler, E. Artacho, J. Gale, A. Garcia, J. Junquera, P. Ordejón, D. Sanchez-Portal, J. Phys. Condens. Matter 14 (2002) 2745–2779.
[32] M. Lin, R. Barnes, D. Torgeson, Phys. Rev. B 24 (1981) 3712–3718.